

Iodine observed in new particle formation events in the Arctic atmosphere during ACCACIA

J. D. Allan^{1,2*}, P. I. Williams^{1,2}, J. Najera¹, J. D. Whitehead¹, M. J. Flynn¹, J. W. Taylor¹, D. Liu¹, E. Darbyshire¹, L. J. Carpenter³, R. Chance³, S. J. Andrews³, S. C. Hackenberg³, and G. McFiggans¹

[1]{School of Earth, Atmospheric and Environmental Sciences, University of Manchester, Oxford Road, Manchester M13 9PL, UK}

[2]{National Centre for Atmospheric Science, University of Manchester, Oxford Road, Manchester M13 9PL, UK}

[3]{Wolfson Atmospheric Chemistry Laboratory, Department of Chemistry, University of York, Heslington, York, YO10 5DD, UK}

Correspondence to: J. D. Allan (james.allan@manchester.ac.uk); tel. +44 161 3068532

Abstract

Accurately accounting for new particle formation (NPF) is crucial to our ability to predict aerosol number concentrations in many environments and thus cloud properties, which is in turn vital in simulating radiative transfer and climate. Here we present an analysis of NPF events observed in the Greenland Sea during the summertime as part of the Aerosol-Cloud Coupling And Climate Interactions in the Arctic (ACCACIA) project. While NPF events have been reported in the Arctic before, we were able, for the first time, to detect iodine in the growing particles using an Aerosol Mass Spectrometer (AMS) during a persistent event in the region of the coastal sea ice near Greenland. Given the potency of iodine as a nucleation precursor, the results imply that iodine was responsible for the initial NPF, a phenomenon that has been reported at lower latitudes and associated with molecular iodine emissions from coastal macroalgae. The initial source of iodine in this instance is not clear, but it was associated with air originating approximately 1 day previously over melting coastal sea ice. These results show that atmospheric models must consider iodine as a source of new particles in addition to established precursors such as sulphur compounds.

1

2 **1 Introduction**

3 In the Arctic, clouds are the dominant factor in the control of the incoming and outgoing
4 energy balance at the Earth's surface and, here and throughout the troposphere, the largest
5 single source of uncertainty in climate predictions. Understanding processes governing
6 atmospheric aerosol concentrations is critically important to improved prediction of clouds
7 and thus weather and climate (Boucher et al., 2013). The optical thickness and lifetime of
8 clouds can be strongly influenced by the population of aerosol particles available to act as
9 cloud condensation nuclei (CCN) (Haywood and Boucher, 2000). Particle concentrations in
10 the summertime Arctic are typically very low (of the order of 10^2 cm^{-3}) and therefore cloud
11 properties in this region are highly sensitive to the mechanisms by which new particles are
12 formed and are grown to viable CCN sizes (roughly 50-100 nm, depending on the cloud
13 conditions) (Merikanto et al., 2009). Understanding these processes is crucial to our
14 predictive capability of climate in the Arctic, as clouds can have a strong warming or cooling
15 effect, depending on a variety of conditions (Hodson et al., 2013).

16 New particle formation (NPF) can dramatically increase aerosol number concentrations in the
17 atmosphere (Kulmala et al., 2004; Spracklen et al., 2006), alongside direct emissions of
18 particles (e.g. through combustion, sea spray, dust suspension etc.), contributing up to half of
19 the global CCN burden (Merikanto et al., 2009; Yu and Luo, 2009). NPF generally occurs
20 through the rapid photochemical production of low vapour pressure secondary material such
21 that stable molecular clusters are able to grow to viable sizes (nm) (Kulmala et al., 2013;
22 Kulmala et al., 2000). As they grow, the freshly nucleated particles act as sinks for the
23 secondary condensable material, potentially shutting off the nucleation process. NPF has been
24 observed in a variety of different environments across the world. The role of sulphuric acid
25 (produced in the atmosphere from the gas phase oxidation of marine biogenic dimethyl
26 sulphide or SO_2 from fossil fuel burning or volcanoes) and organic matter (chiefly from
27 terrestrial biogenic sources) has been extensively studied (e.g. Laaksonen et al., 2008; Zhang
28 et al., 2004a; Riccobono et al., 2014) and it has also been shown that ammonia and amines
29 have very important roles in promoting NPF through ternary processes (Kirkby et al., 2011;
30 Almeida et al., 2013; Berndt et al., 2014).

31 Because of the generally low CCN number concentrations present, the Arctic atmosphere is
32 highly sensitive to NPF. This in turn means that predictions of CCN are highly sensitive to the

1 processes responsible for NPF, which are currently highly uncertain in this environment (Lee
2 et al., 2012). NPF has previously been observed during Arctic ship-based measurements and
3 given the lack of significant biogenic or anthropogenic sources of organic precursors, most
4 efforts to model these observations have only invoked NPF from the oxidation of sulphur
5 species (Korhonen et al., 2008). An alternative hypothesis is that rather than nucleation, the
6 initial source of the new particles is the fission of organic biogels (aggregations of biological
7 macromolecules) in primary particles (Karl et al., 2013; Karl et al., 2012).

8 In coastal environments at lower latitudes, frequent daytime NPF events have been observed
9 associated with gaseous iodine at low tide. This suggests that in these environments, iodine is
10 the dominant source of nanoparticles, which have been observed to grow to larger sizes able
11 to scatter radiation and contribute to CCN (McFiggans et al., 2004; McFiggans et al., 2010;
12 O'Dowd et al., 2002; Whitehead et al., 2009; Yoon et al., 2006; Lehtipalo et al., 2010).
13 Gaseous I₂ is produced in abundance by macroalgae species (*Laminaria digitata*, *Fucus*
14 *vesiculosus* and *Ascophyllum nodosum* have been identified as being responsible for NPF) in
15 response to being exposed to the atmosphere (Küpper et al., 2008; Huang et al., 2013) and is
16 rapidly photooxidised to iodine monoxide (IO) and higher iodine oxides, which polymerise to
17 form particles (Saiz-Lopez et al., 2012; Saunders et al., 2010). To date, iodine-initiated NPF
18 has most commonly been observed in seaweed-rich coastal areas but the theoretical potential
19 exists in low background aerosol conditions with associated high iodine fluxes (Mahajan et
20 al., 2010). Atkinson et al. (2012) attributed NPF events observed in the Weddell Sea in
21 Antarctica to iodine emissions from sea ice, although no data on aerosol composition was
22 presented.

23 Here we present data on NPF events recorded aboard the RRS James Clark Ross in the
24 Greenland Sea during the summer ACCACIA cruise. Through the analysis of a particularly
25 strong and persistent case study, we show evidence for the role of iodine in NPF events in this
26 region.

27

28 **2 Methods**

29 As part of the Aerosol-Cloud Coupling And Climate Interactions in the Arctic (ACCACIA)
30 project, intensive measurements of aerosol composition and properties were made aboard the
31 RRS *James Clark Ross*, an ice-hardened research vessel. The cruise (JR288) consisted of a

1 number of traverses in and out of the sea ice margin in the region of Greenland and Svalbard
2 during July and August 2013 (see Fig. 1).

3 The University of Manchester instrumentation was located in an instrumented sea container
4 on the foredeck of the *James Clark Ross*, sampling air through a 5 metre stack via a 3.5 μm
5 cut cyclone, as has been performed during previous measurement campaigns (Allan et al.,
6 2009). No attempt to correct for size-dependent particle losses has been made for this work,
7 as it will not affect the qualitative results presented here. No in-line drier was used, as the
8 relative humidity (RH) in the container was maintained low due to the temperature
9 differential. A number of instruments sub-sampled from the main inlet manifold.

10 A Differential Mobility Particle Sizer (DMPS) system was used to measure size-resolved
11 particle number concentrations. This was built at the University of Manchester (Williams et
12 al., 2007) using dual ‘Vienna’ design Differential Mobility Analysers (DMAs) (Winklmayr et
13 al., 1991) of different lengths (to cover different particle size ranges) with stepping voltages,
14 selecting negatively-charged particles. TSI (Shoreview, MN, USA) model 3010 and 3025a
15 Condensation Particle Counters (CPCs) were used to count the particles and the Wiedensohler
16 (1988) charging parameterisation used to invert the data. The sheath air system uses a
17 recirculating system dried to a low (<20% RH) humidity using a membrane drier linked to a
18 dry compressed air system. Total number concentrations were provided by a TSI model 3776
19 CPC.

20 An Aerodyne (Billerica, MA, USA) Aerosol Mass Spectrometer (AMS) of the High
21 Resolution Time-of-Flight (HR-TOF) design (Canagaratna et al., 2007) was also used to
22 measure particle composition. Calibrations were performed using monodisperse ammonium
23 nitrate for mass and NIST-certified Polystyrene Latex (PSL) Spheres (Thermo Scientific) for
24 size. The data was collected in ‘V’ and ‘W’ mass spectral modes, which have $m/\Delta m$
25 resolutions of 2100 and 4300 at $m/z=200$ respectively (DeCarlo et al., 2006), although only
26 ‘V’ mode data is presented here due because of the low signal-to-noise ratio of the ‘W’ mode
27 data.

28 A Droplet Measurement Technologies (Boulder, CO, USA) Single Particle Soot Photometer
29 (SP2) was used to measure black carbon. This was a version ‘D’ instrument, calibrated using
30 monodisperse Aquadag, scaled by a factor of 0.75 as recommended by Laborde et al. (2012)

31 Sub-saturated particle growth factors were measured using a Hygroscopicity Tandem
32 Differential Mobility Analyser (HTDMA). This was the second Manchester-built instrument

1 (Whitehead et al., 2014), conforming to EUSAAR specifications (Duplissy et al., 2009). This
2 uses two Brechtel Manufacturing Inc. (Hayward, CA, USA) DMAs housed in temperature-
3 controlled boxes and linked in series. The first had dry sheath air (<20% RH) while the sheath
4 air in the second was maintained at 90% RH, using a membrane humidification system on a
5 feedback loop with an Edgetech (Marlborough, MA, USA) dew point monitor. The particles
6 were counted using a TSI model 3782 water-based CPC. Sizes were calibrated with PSL
7 spheres and humidity was validated through the comparison of the measured deliquescence
8 humidities of ammonium sulphate and sodium chloride with modelled values (Topping et al.,
9 2005). Data were inverted using the method of Gysel et al. (2009).

10 Halocarbons were quantified in air and seawater using two Agilent 6850 gas chromatographs
11 (GC) with 5975C mass selective detectors (MSDs) coupled to commercial thermal desorption
12 units (TD, Markes Unity2-CIA8) in a system described by Andrews et al. (2015). One
13 instrument was dedicated to air analysis and the other to water, and both instruments were
14 calibrated daily for halocarbons using NOAA gas standard SX-3570 (Jones et al., 2011).
15 Instrument drift was corrected for during (air analyses) or after (water analyses) each sample
16 using atmospheric carbon tetrachloride as an internal standard. Underway seawater samples
17 were collected from the pumped non-toxic seawater supply of the ship using a semi-
18 automated purge and trap system plumbed directly into the underway supply. The sample
19 lines and valves were flushed with underway water before each sample. 20 mL water samples
20 was pumped into the purge vessel (2 minute sampling time) and purged with 1 L of zero-
21 grade nitrogen gas. Purge efficiencies were $100 \pm 2\%$ for bromocarbons and $90 \pm 10\%$ for
22 iodocarbons. All water samples were passed through an in-line pre-combusted grade GF/F
23 filter. A bake-out program was also run between each pair of air and water samples. The
24 duration of each sampling cycle (air-water-bake) was 65 minutes.

25 Back trajectory analysis was performed using HYSPLIT 4 (Draxler and Hess, 1998),
26 employing GDAS reanalysis wind fields (NOAA Air Resources Laboratory, Boulder, CO,
27 USA). Back trajectories were started at 20 m above mean sea level and run using modelled
28 vertical velocities.

29

30 **3 Results**

31 During the measurements, a number of events were noted in the DMPS data whereby a large
32 number of small particles contributed dramatically to the ambient population. Contributions

1 from combustion sources (e.g. ship plumes) were eliminated by the lack of black carbon (BC)
2 detectable by the SP2. The data were also filtered according to short-lived spikes seen with
3 the CPC that could be associated with other sources from within the ship. The DMPS
4 occasionally showed ‘open’ distributions, whereby the peak existed at or below the lower size
5 limit of the instrument (3 nm), providing evidence for NPF (Fig. 2). Time periods where a
6 significant portion of the detected particles were smaller than 10 nm are identified on Fig. 1a,
7 on an overlay of the cruise track and sea ice concentration data using the polar stereographic
8 product from the Special Sensor Microwave Imager/Sounder (SSMIS) instrument on the
9 Defense Meteorological Satellite Program (DMSP) F17 platform (Cavaliere et al., 2013).

10 These periods all occurred in proximity to coastal locations around Iceland, Greenland and
11 Svalbard and the influence of terrestrial air is seen in the lowering of the RH in Fig 2, which
12 is otherwise close to saturation. The most significant and persistent of these events occurred
13 between the 25th and 27th of July, when the ship was close to the sea ice margin off the coast
14 of northeastern Greenland and the air had previously travelled over the breaking sea ice off
15 Greenland. (Fig. 1b). Markers for microalgal activity in the form of CH₂Br₂ were also
16 observed to be elevated during this period (Fig 1c). During this period, the nonrefractory
17 aerosol composition was mainly organic, with only around 0.1 µg m⁻³ of sulphate present
18 (Fig. 3).

19 The candidate NPF events were also associated with elevated number concentrations, with
20 transitions over periods of hours (Figs. 2 and 4), indicating that the new particles last long
21 enough to grow to the larger sizes that can contribute to CCN. It is likely that the transitions
22 in the size distributions resulted from changes to the source footprint in relation to the
23 position of the ship rather than in situ growth of the observed new particles. While the growth
24 events reported here may seem to resemble the characteristic ‘banana’ events observed at
25 coastal sites and other locations (Kulmala et al., 2004; Ehn et al., 2010; Yli-Juuti et al., 2011),
26 they differ in the following behaviour: 1) There are breaks in the growth observed (e.g. 25 Jul
27 00:00) 2) The apparent growth around 26 Jul 20:00 is exponential rather than linear in
28 diameter space 3) The growth apparently reverses at 26 Jul 00:30 and 27 Jul 09:00. It is worth
29 noting that the previously reported behaviours result from the diurnal modulation of boundary
30 layer dynamics and photochemistry caused by the local day-night cycle in conjunction with a
31 stable source footprint. This is not the case here, due to continuous insolation and reduced
32 dynamics of the marine boundary layer, combined with a varying source footprint (due to the

1 movement of the ship and varying wind direction). Therefore, analogies with the temporal
2 behaviour at other locations cannot necessarily be drawn.

3 Aerosol Mass Spectrometer (AMS) data during the 25-27th July showed a signal at $m/z=127$
4 during the periods when larger particles were present (Fig. 4), which is identified as I^+ ions by
5 its precise mass/charge ratio of 126.90 (Fig. S1.1) (Wang et al., 2012). I^+ has previously been
6 reported as the largest peak in photochemically-produced iodine oxide AMS mass spectra in
7 the laboratory (McFiggans et al., 2004; Jimenez et al., 2003), but this is the first time that it
8 has been reported in ambient particles. In previous coastal studies, owing to the proximity to
9 the initial source of iodine, particles did not grow to sizes large enough (around 30 nm) to be
10 transmitted by the AMS aerodynamic lens inlet (Liu et al., 2007; Zhang et al., 2004b; Zhang
11 et al., 2004a). In this study, the particles grew to sufficient sizes, however it should be noted
12 that the AMS is still not able to observe iodine during the periods where the particles were
13 smaller than this, so does not see iodine during the very early stages of growth.

14 To investigate whether the I^+ signal could be associated with processes governing the
15 formation of organic aerosols (Fig. 3.), Positive Matrix Factorisation (PMF) was performed
16 on the data (Paatero and Tapper, 1994; Ulbrich et al., 2009). This assigns the organic mass to
17 different ‘factors’ according to the temporal behaviour of the mass spectral matrix and is
18 detailed in section 2 of the supplementary material. Once shipping emissions and
19 misattributed sea salt are excluded, this analysis found that the organic matter detected by the
20 AMS could be attributed to methyl sulphonic acid (MSA) (Phinney et al., 2006; Decesari et
21 al., 2011) and highly-oxygenated organic material (McFiggans et al., 2005; Jimenez et al.,
22 2009). The I^+ signal was not represented in any of the factors derived, only manifested in the
23 residual data, which implies that the particulate iodine had a source that was distinct from the
24 processes controlling the formation of particulate organic matter (be they primary or
25 secondary). A further implication of the MSA observation is that this compound was at least
26 partly responsible for the reported sulphate concentrations, as this also produces SO^+ and
27 SO_2^+ ions in the mass spectrum (Zorn et al., 2008). Therefore, the actual non-seasalt sulphate
28 concentration is likely to be lower than what is reported, but the quantitative fraction of MSA
29 is difficult to estimate, as the fragmentation behaviour is highly variable and not calibrated
30 during this study.

31

1 4 Discussion

2 To link the I^+ signals detected by the AMS to the particles seen by the DMPS, the size-
3 resolved data from the two instruments were quantitatively compared through the fitting of
4 lognormal distributions. Shown in Fig. 5 are the DMPS volume-weighted size distributions
5 from the period of peak I^+ concentrations (26 July 22:50-23:45 UTC), together with the AMS
6 Particle Time-of-Flight size-resolved data for I^+ , organics and sulphate. The AMS data was of
7 a low signal-to-noise ratio, due to the short averaging time and low signal levels (Allan et al.,
8 2003), however the fits converged consistently using a standard Levenberg-Marquardt
9 algorithm, with the peak centres, widths and heights allowed to vary freely. The DMPS
10 distribution is bimodal, with the Aitken mode related to the I^+ peak in the AMS data and the
11 accumulation mode related to the sulphate and organic modes. The ratio of the fitted Aitken
12 mode diameters yields a particle effective density of $1.77 \pm 0.23 \text{ g cm}^{-3}$, which is typical of an
13 inorganic aerosol (Cross et al., 2007). Given that this quantity is a product of the material
14 density and the Jayne shape factor (DeCarlo et al., 2004; Jayne et al., 2000), this may be an
15 underestimate of the material density if the particles are nonspherical, as has been suggested
16 by electron microscopy of laboratory-generated particles (McFiggans et al., 2004).

17 The shift in composition of these particles is also reflected in the HTDMA data, which shows
18 that during this period, the growth factor of 50 nm dry particles at 90 % RH is 1.34, whereas
19 for the rest of the cruise, values were always greater than 1.5 (Fig. 6). The low growth factor
20 and the density estimate are consistent with iodine oxide making up a significant portion of
21 the particulate volume; I_2O_5 has a material density of 5 g cm^{-3} and laboratory studies have
22 shown iodine oxide particles to exhibit low growth factors (Jimenez et al., 2003; McFiggans
23 et al., 2004; Murray et al., 2012). This is different to what would be expected of organic
24 matter, which tends to be of a low density and low growth factor, and inorganic salts and
25 sulphuric acid, which are high density and high growth factor (Cross et al., 2007; Gysel et al.,
26 2007).

27 While the data discussed above provides strong evidence for the presence of iodine in the
28 particles during these events, it does not prove that iodine was responsible for the initial NPF,
29 which will have occurred upwind prior to measurement. However, given the rapidity of the
30 iodine oxidation process and the very low volatility of the products (McFiggans et al., 2010;
31 Whitehead et al., 2009; Lehtipalo et al., 2010), it is reasonable to assume that the presence of
32 iodine-based secondary particulate matter implies that iodine-initiated NPF was also

1 occurring. It is also worth noting that sulphate concentrations were low during the main case
2 study, so this NPF event did not occur during a period of particularly strong sulphuric acid
3 production.

4 In situ sea-air fluxes and atmospheric mixing ratios of iodocarbons (CH_3I , CH_2I_2 and CH_2ICl)
5 measured during the NPF event were very low ($< 2 \text{ nmol m}^{-2} \text{ d}^{-1}$ and $\approx 0.5 \text{ pptv}$ for CH_3I ; $<$
6 $1 \text{ nmol m}^{-2} \text{ d}^{-1}$ and $< 0.02 \text{ pptv}$ for both CH_2I_2 and CH_2ICl , see Fig. S1.2). Although these
7 compounds are found in sea-ice (Atkinson et al., 2012; Granfors et al., 2014) and have been
8 shown to cause NPF in the laboratory (Jimenez et al., 2003), the iodocarbon emissions and
9 atmospheric concentrations found in this and earlier studies are insufficient to sustain the very
10 high local concentrations of IO required for iodine nucleation (McFiggans et al., 2004),
11 suggesting the gaseous precursor may have been an inorganic form of iodine such as I_2 .

12 The initial source of the iodine responsible for these events is not known. Macroalgae have
13 been identified as a molecular iodine source in midlatitude coastal studies (Küpper et al.,
14 2008; Huang et al., 2013) and macroalgae beds containing kelps and wracks also occur on the
15 northeast coast of Greenland (Borum et al., 2002), albeit with a different species composition.
16 Elevated CH_2Br_2 levels would be consistent with a macroalgal source (e.g. Laturnus, 1996).
17 However, the biomass density of the north-east Greenland kelp beds may be considerably less
18 than found at temperate locations such as Galway Bay (Werner and Kraan, 2004), and ice
19 scouring may reduce macroalgal density in shallower waters where the algae are more likely
20 to be exposed to the atmosphere (Wiencke and Amsler, 2012; Borum et al., 2002).

21 A source of inorganic iodine from the marginal sea-ice zone is plausible, and would be
22 consistent with the findings of Atkinson et al. (2012). Microalgae, particularly diatoms, may
23 be considered as a potential source of iodine in this region. Diatoms are prominent members
24 of microalgal blooms occurring at the receding ice edge, and also in communities growing
25 within the ice itself. Ice diatoms have previously been shown to be a potential direct source of
26 HOI and I_2 to the Arctic atmosphere (Hill and Manley, 2009). The presence of elevated levels
27 of CH_2Br_2 in air compared to levels in seawater during the iodine particle event (Fig 1c) is
28 consistent with this suggestion, as polar diatoms are known to be a strong source of
29 bromocarbons (Sturges et al., 1992; Sturges et al., 1993). Note that it is not expected that the
30 observed bromocarbons directly participate in the NPF; the molecules are too small to form
31 low volatility organic oxidation products and bromine, unlike iodine, does not form a series of

1 stable condensed-phase oxides. Furthermore, there was no trace of any bromine-containing
2 signal in the AMS data.

3 I₂ and HOI may also be formed by the abiotic oxidation of iodide, either by gaseous ozone on
4 the sea surface (Carpenter et al., 2013), or within sea-ice brine channels followed by
5 emissions from the quasi-liquid layer on the surface of the sea-ice (Saiz-Lopez et al., 2015).
6 High levels of iodide associated with biological activity in the sea ice region have sometimes
7 been observed (Chance et al., 2010). More recently, microalgal aggregates released from
8 melting sea-ice have also been proposed as an iodide source (Assmy et al., 2013; Boetius et
9 al., 2013). Although such aggregates were not observed from the ship during this work, given
10 that the initial source of the iodine was upwind, the possibility this was an iodine source is
11 not ruled out. (Indeed, we note previous observations of elevated iodide associated with
12 microalgal aggregates were made at higher latitudes than the ship position during the NPF
13 event). An additional suggestion for the source of iodine is chemical production from the ice
14 surface itself, promoted by the freezing of sea salt in the presence of nitrite ions (O'Driscoll et
15 al., 2006). It should be noted that no NPF events were recorded near the ice margin to the
16 northeast of Svalbard during the latter stages of the cruise, so it may be that the phenomenon
17 observed here is restricted to coastal areas or certain stages of the ice melt process.

18

19 **5 Conclusions**

20 Herein we show observations of new particle formation (NPF) over the Greenland Sea in
21 summer. A long-lasting event, associated with air originating over the breaking sea ice off
22 Greenland, featured NPF and particles growing to sizes in excess of 50 nm. During this
23 period, iodine was unambiguously detected by an Aerodyne Aerosol Mass Spectrometer.
24 Furthermore, measurements of hygroscopicity and effective density were consistent with
25 iodine oxide comprising a significant portion of the particulate volume. This strongly implies
26 that iodine had a role in the initial NPF events, which is a phenomenon previously associated
27 with coastal locations at lower latitudes (Huang et al., 2013; McFiggans et al., 2010;
28 McFiggans et al., 2004). The initial source of the iodine in this case is unlikely to be the
29 macroalgae identified during previous studies, but could be speculatively related to other
30 macroalgae species or microalgae associated with the sea ice, which would be consistent with
31 the findings of Atkinson et al. (2012) based on measurements in Antarctica.

1 These results show that correct prediction of Arctic aerosol number concentrations requires
2 knowledge of iodine processes in new particle nucleation and growth. Our observations
3 suggest that the source of iodine is related to processes associated with coastal sea ice, so this
4 could represent a potentially significant source of particles during periods of ice loss and thus
5 a potential climate feedback mechanism. As yet we have insufficient data to predict how
6 widespread these processes are, but if this phenomenon is limited to coastal areas, it would
7 not explain the events above 80 °N studied by Karl et al. (2012). More work is required to
8 identify the initial source of the iodine and the exact mechanisms for iodine NPF at a
9 molecular level (Kulmala et al., 2013).

10

11 **Data Availability**

12 Processed data are archived at the British Atmospheric Data Centre ACCACIA archive. Raw
13 data available on request.

14

15 **Acknowledgements**

16 This work was supported by the UK Natural Environment Research Council through the
17 Aerosol-Cloud Coupling And Climate Interactions in the Arctic (ACCACIA) project (Grant
18 refs: NE/I028696/1; NE/I028769/1) and a PhD studentship (E. Darbyshire). For the cruise
19 planning, operation and support, the authors thank the British Antarctic Survey (BAS), the
20 crew of the RRS *James Clark Ross* and Prof. Ian Brooks (U. Leeds) as PI of ACCACIA.
21 Coastline data were obtained from the National Geophysical Data Centre (Boulder, CO,
22 USA). Sea ice data was obtained from the NASA Distributed Active Archive Center at the
23 National Snow and Ice Data Center (Boulder, CO USA).

24

25 **References**

26 Allan, J. D., Jimenez, J. L., Williams, P. I., Alfarra, M. R., Bower, K. N., Jayne, J. T., Coe,
27 H., and Worsnop, D. R.: Quantitative sampling using an Aerodyne aerosol mass spectrometer
28 - 1. Techniques of data interpretation and error analysis, *J. Geophys. Res.-Atmos.*, 108, 4090,
29 doi:10.1029/2002JD002358, 2003.

1 Allan, J. D., Topping, D. O., Good, N., Irwin, M., Flynn, M., Williams, P. I., Coe, H., Baker,
2 A. R., Martino, M., Niedermeier, N., Wiedensohler, A., Lehmann, S., Muller, K., Herrmann,
3 H., and McFiggans, G.: Composition and properties of atmospheric particles in the eastern
4 Atlantic and impacts on gas phase uptake rates, *Atmos. Chem. Phys.*, 9, 9299-9314, 2009.

5 Almeida, J., Schobesberger, S., Kurten, A., Ortega, I. K., Kupiainen-Maatta, O., Praplan, A.
6 P., Adamov, A., Amorim, A., Bianchi, F., Breitenlechner, M., David, A., Dommen, J.,
7 Donahue, N. M., Downard, A., Dunne, E., Duplissy, J., Ehrhart, S., Flagan, R. C., Franchin,
8 A., Guida, R., Hakala, J., Hansel, A., Heinritzi, M., Henschel, H., Jokinen, T., Junninen, H.,
9 Kajos, M., Kangasluoma, J., Keskinen, H., Kupc, A., Kurten, T., Kvashin, A. N., Laaksonen,
10 A., Lehtipalo, K., Leiminger, M., Leppa, J., Loukonen, V., Makhmutov, V., Mathot, S.,
11 McGrath, M. J., Nieminen, T., Olenius, T., Onnela, A., Petaja, T., Riccobono, F., Riipinen, I.,
12 Rissanen, M., Rondo, L., Ruuskanen, T., Santos, F. D., Sarnela, N., Schallhart, S.,
13 Schnitzhofer, R., Seinfeld, J. H., Simon, M., Sipila, M., Stozhkov, Y., Stratmann, F., Tome,
14 A., Trostl, J., Tsagkogeorgas, G., Vaattovaara, P., Viisanen, Y., Virtanen, A., Vrtala, A.,
15 Wagner, P. E., Weingartner, E., Wex, H., Williamson, C., Wimmer, D., Ye, P. L., Yli-Juuti,
16 T., Carslaw, K. S., Kulmala, M., Curtius, J., Baltensperger, U., Worsnop, D. R., Vehkamäki,
17 H., and Kirkby, J.: Molecular understanding of sulphuric acid-amine particle nucleation in the
18 atmosphere, *Nature*, 502, 359-363, Doi 10.1038/Nature12663, 2013.

19 Andrews, S. J., Hackenberg, S. C., and Carpenter, L. J.: Technical Note: A fully automated
20 purge and trap GC-MS system for quantification of volatile organic compound (VOC) fluxes
21 between the ocean and atmosphere, *Ocean Sci.*, 11, 313-321, doi:10.5194/os-11-313-2015,
22 2015..

23 Assmy, P., Ehn, J. K., Fernandez-Mendez, M., Hop, H., Katlein, C., Sundfjord, A., Bluhm,
24 K., Daase, M., Engel, A., Fransson, A., Granskog, M. A., Hudson, S. R., Kristiansen, S.,
25 Nicolaus, M., Peeken, I., Renner, A. H. H., Spreen, G., Tatarek, A., and Wiktor, J.: Floating
26 Ice-Algal Aggregates below Melting Arctic Sea Ice, *Plos One*, 8, ARTN e76599, DOI
27 10.1371/journal.pone.0076599, 2013.

28 Atkinson, H. M., Huang, R. J., Chance, R., Roscoe, H. K., Hughes, C., Davison, B.,
29 Schönhardt, A., Mahajan, A. S., Saiz-Lopez, A., Hoffmann, T., and Liss, P. S.: Iodine
30 emissions from the sea ice of the Weddell Sea, *Atmos. Chem. Phys.*, 12, 11229-11244,
31 10.5194/acp-12-11229-2012, 2012.

1 Berndt, T., Sipila, M., Stratmann, F., Petaja, T., Vanhanen, J., Mikkila, J., Patokoski, J.,
2 Taipale, R., Mauldin, R. L., and Kulmala, M.: Enhancement of atmospheric H₂SO₄/H₂O
3 nucleation: organic oxidation products versus amines, *Atmos. Chem. Phys.*, 14, 751-764, DOI
4 10.5194/acp-14-751-2014, 2014.

5 Boetius, A., Albrecht, S., Bakker, K., Bienhold, C., Felden, J., Fernandez-Mendez, M.,
6 Hendricks, S., Katlein, C., Lalande, C., Krumpen, T., Nicolaus, M., Peeken, I., Rabe, B.,
7 Rogacheva, A., Rybakova, E., Somavilla, R., Wenzhofer, F., and Sc, R. P. A.-.-S.: Export of
8 Algal Biomass from the Melting Arctic Sea Ice, *Science*, 339, 1430-1432, DOI
9 10.1126/science.1231346, 2013.

10 Borum, J., Pedersen, M. F., Krause-Jensen, D., Christensen, P. B., and Nielsen, K.: Biomass,
11 photosynthesis and growth of *Laminaria saccharina* in a high-arctic fjord, NE Greenland, *Mar*
12 *Biol*, 141, 11-19, DOI 10.1007/s00227-002-0806-9, 2002.

13 Boucher, O., Randall, D., Artaxo, P., Bretherton, C., Feingold, G., Forster, P., Kerminen, V.
14 M., Kondo, Y., liao, H., lohmann, U., Rasch, P., Satheesh, S. K., Sherwood, S., Stevens, B.,
15 and Zhang, X. Y.: Clouds and Aerosols, in: *Climate Change 2013: The Physical Science*
16 *Basis. Contribution of Working Group I to the Fifth Assessment Report of the*
17 *Intergovernmental Panel on Climate Change*, edited by: Stocker, T. F., Qin, D., Plattner, G.
18 K., Tignor, M., Allen, S. K., Boschung, J., Nauels, A., Xia, Y., Bex, V., and Midgley, P. M.,
19 Cambridge University Press, Cambridge, United Kingdom; New York, NY, USA., 2013.

20 Canagaratna, M. R., Jayne, J. T., Jimenez, J. L., Allan, J. D., Alfarra, M. R., Zhang, Q.,
21 Onasch, T. B., Drewnick, F., Coe, H., Middlebrook, A., Delia, A., Williams, L. R., Trimborn,
22 A. M., Northway, M. J., DeCarlo, P. F., Kolb, C. E., Davidovits, P., and Worsnop, D. R.:
23 Chemical and microphysical characterization of ambient aerosols with the aerodyne aerosol
24 mass spectrometer, *Mass Spectrom. Rev.*, 26, 185-222, Doi 10.1002/Mas.20115, 2007.

25 Carpenter, L. J., MacDonald, S. M., Shaw, M. D., Kumar, R., Saunders, R. W., Parthipan, R.,
26 Wilson, J., and Plane, J. M. C.: Atmospheric iodine levels influenced by sea surface emissions
27 of inorganic iodine, *Nat Geosci*, 6, 108-111, Doi 10.1038/Ngeo1687, 2013.

28 Cavalieri, D., Parkinson, C., Gloersen, P., and Zwally., H. J.: Sea Ice Concentrations from
29 Nimbus-7 SMMR and DMSP SSM/I-SSMIS Passive Microwave Data.
30 [nt_20130726_f17_v01_n], NASA DAAC at the National Snow and Ice Data Center,
31 Boulder, Colorado USA, 2013.

1 Chance, R., Weston, K., Baker, A. R., Hughes, C., Malin, G., Carpenter, L., Meredith, M. P.,
2 Clarke, A., Jickells, T. D., Mann, P., and Rossetti, H.: Seasonal and interannual variation of
3 dissolved iodine speciation at a coastal Antarctic site, *Mar. Chem.*, 118, 171-181, DOI
4 10.1016/j.marchem.2009.11.009, 2010.

5 Cross, E. S., Slowik, J. G., Davidovits, P., Allan, J. D., Worsnop, D. R., Jayne, J. T., Lewis,
6 D. K., Canagaratna, M., and Onasch, T. B.: Laboratory and ambient particle density
7 determinations using light scattering in conjunction with aerosol mass spectrometry, *Aerosol*
8 *Sci. Technol.*, 41, 343-359, 2007.

9 DeCarlo, P. F., Slowik, J. G., Worsnop, D. R., Davidovits, P., and Jimenez, J. L.: Particle
10 Morphology and Density Characterization by Combined Mobility and Aerodynamic Diameter
11 Measurements. Part 1: Theory, *Aerosol Sci. Technol.*, 38, 1185–1205, 2004.

12 DeCarlo, P. F., Kimmel, J. R., Trimborn, A., Northway, M. J., Jayne, J. T., Aiken, A. C.,
13 Gonin, M., Fuhrer, K., Horvath, T., Docherty, K. S., Worsnop, D. R., and Jimenez, J. L.:
14 Field-deployable, high-resolution, time-of-flight aerosol mass spectrometer, *Anal. Chem.*, 78,
15 8281-8289, 10.1021/ac061249n, 2006.

16 Decesari, S., Finessi, E., Rinaldi, M., Paglione, M., Fuzzi, S., Stephanou, E. G., Tziaras, T.,
17 Spyros, A., Ceburnis, D., O'Dowd, C., Dall'Osto, M., Harrison, R. M., Allan, J., Coe, H., and
18 Facchini, M. C.: Primary and secondary marine organic aerosols over the North Atlantic
19 Ocean during the MAP experiment, *J. Geophys. Res.-Atmos.*, 116, Artn D22210, Doi
20 10.1029/2011jd016204, 2011.

21 Draxler, R. R., and Hess, G. D.: An overview of the HYSPLIT_4 modeling system of
22 trajectories, dispersion, and deposition., *Aust. Meteor. Mag.*, 47, 295-308, 1998.

23 Duplissy, J., Gysel, M., Sjogren, S., Meyer, N., Good, N., Kammermann, L., Michaud, V.,
24 Weigel, R., Martins dos Santos, S., Gruening, C., Villani, P., Laj, P., Sellegri, K., Metzger,
25 A., McFiggans, G. B., Wehrle, G., Richter, R., Dommen, J., Ristovski, Z., Baltensperger, U.,
26 and Weingartner, E.: Intercomparison study of six HTDMAs: results and recommendations,
27 *Atmos. Meas. Tech.*, 2, 363-378, 10.5194/amt-2-363-2009, 2009.

28 Ehn, M., Vuollekoski, H., Petaja, T., Kerminen, V. M., Vana, M., Aalto, P., de Leeuw, G.,
29 Ceburnis, D., Dupuy, R., O'Dowd, C. D., and Kulmala, M.: Growth rates during coastal and
30 marine new particle formation in western Ireland, *J. Geophys. Res.-Atmos.*, 115, Artn
31 D18218, 10.1029/2010jd014292, 2010.

1 Granfors, A., Ahnoff, M., Mills, M. M., and Abrahamsson, K.: Organic iodine in Antarctic
2 sea ice: A comparison between winter in the Weddell Sea and summer in the Amundsen Sea,
3 *J. Geophys. Res.-Biogeo*, 119, 2014JG002727, 10.1002/2014JG002727, 2014.

4 Gysel, M., Crosier, J., Topping, D. O., Whitehead, J. D., Bower, K. N., Cubison, M. J.,
5 Williams, P. I., Flynn, M. J., McFiggans, G. B., and Coe, H.: Closure study between chemical
6 composition and hygroscopic growth of aerosol particles during TORCH2, *Atmos. Chem.*
7 *Phys.*, 7, 6131–6144, 2007.

8 Gysel, M., McFiggans, G. B., and Coe, H.: Inversion of tandem differential mobility analyser
9 (TDMA) measurements, *J. Aerosol. Sci.*, 40, 134-151, DOI 10.1016/j.jaerosci.2008.07.013,
10 2009.

11 Haywood, J., and Boucher, O.: Estimates of the direct and indirect radiative forcing due to
12 tropospheric aerosols: A review, *Rev. Geophys.*, 38, 513-543, 10.1029/1999RG000078, 2000.

13 Hill, V. L., and Manley, S. L.: Release of reactive bromine and iodine from diatoms and its
14 possible role in halogen transfer in polar and tropical oceans, *Limnol Oceanogr*, 54, 812-822,
15 DOI 10.4319/lo.2009.54.3.0812, 2009.

16 Hodson, D. R., Keeley, S. E., West, A., Ridley, J., Hawkins, E., and Hewitt, H.: Identifying
17 uncertainties in Arctic climate change projections, *Clim Dynam*, 40, 2849-2865,
18 10.1007/s00382-012-1512-z, 2013.

19 Huang, R. J., Thorenz, U. R., Kundel, M., Venables, D. S., Ceburnis, D., Ho, K. F., Chen, J.,
20 Vogel, A. L., Kupper, F. C., Smyth, P. P. A., Nitschke, U., Stengel, D. B., Berresheim, H.,
21 O'Dowd, C. D., and Hoffmann, T.: The seaweeds *Fucus vesiculosus* and *Ascophyllum*
22 *nodosum* are significant contributors to coastal iodine emissions, *Atmos. Chem. Phys.*, 13,
23 5255-5264, DOI 10.5194/acp-13-5255-2013, 2013.

24 Jayne, J. T., Leard, D. C., Zhang, X. F., Davidovits, P., Smith, K. A., Kolb, C. E., and
25 Worsnop, D. R.: Development of an aerosol mass spectrometer for size and composition
26 analysis of submicron particles, *Aerosol Sci. Technol.*, 33, 49-70, 10.1080/027868200410840,
27 2000.

28 Jimenez, J. L., Bahreini, R., Cocker, D. R., Zhuang, H., Varutbangkul, V., Flagan, R. C.,
29 Seinfeld, J. H., O'Dowd, C. D., and Hoffmann, T.: New particle formation from
30 photooxidation of diiodomethane (CH₂I₂), *J. Geophys. Res.-Atmos.*, 108, 4318,
31 doi:10.1029/2002JD002452, 2003.

1 Jimenez, J. L., Canagaratna, M. R., Donahue, N. M., Prevot, A. S. H., Zhang, Q., Kroll, J. H.,
2 DeCarlo, P. F., Allan, J. D., Coe, H., Ng, N. L., Aiken, A. C., Docherty, K. S., Ulbrich, I. M.,
3 Grieshop, A. P., Robinson, A. L., Duplissy, J., Smith, J. D., Wilson, K. R., Lanz, V. A.,
4 Hueglin, C., Sun, Y. L., Tian, J., Laaksonen, A., Raatikainen, T., Rautiainen, J., Vaattovaara,
5 P., Ehn, M., Kulmala, M., Tomlinson, J. M., Collins, D. R., Cubison, M. J., E, Dunlea, J.,
6 Huffman, J. A., Onasch, T. B., Alfarra, M. R., Williams, P. I., Bower, K., Kondo, Y.,
7 Schneider, J., Drewnick, F., Borrmann, S., Weimer, S., Demerjian, K., Salcedo, D., Cottrell,
8 L., Griffin, R., Takami, A., Miyoshi, T., Hatakeyama, S., Shimono, A., Sun, J. Y., Zhang, Y.
9 M., Dzepina, K., Kimmel, J. R., Sueper, D., Jayne, J. T., Herndon, S. C., Trimborn, A. M.,
10 Williams, L. R., Wood, E. C., Middlebrook, A. M., Kolb, C. E., Baltensperger, U., and
11 Worsnop, D. R.: Evolution of Organic Aerosols in the Atmosphere, *Science*, 326, 1525-1529,
12 10.1126/science.1180353, 2009.

13 Jones, C. E., Andrews, S. J., Carpenter, L. J., Hogan, C., Hopkins, F. E., Laube, J. C.,
14 Robinson, A. D., Spain, T. G., Archer, S. D., Harris, N. R. P., Nightingale, P. D., O'Doherty,
15 S. J., Oram, D. E., Pyle, J. A., Butler, J. H., and Hall, B. D.: Results from the first national UK
16 inter-laboratory calibration for very short-lived halocarbons, *Atmos. Meas. Tech.*, 4, 865-874,
17 10.5194/amt-4-865-2011, 2011.

18 Karl, M., Leck, C., Gross, A., and Pirjola, L.: A study of new particle formation in the marine
19 boundary layer over the central Arctic Ocean using a flexible multicomponent aerosol
20 dynamic model, *Tellus B*, 64, 17158, Doi 10.3402/Tellusb.V64i0.17158, 2012.

21 Karl, M., Leck, C., Coz, E., and Heintzenberg, J.: Marine nanogels as a source of atmospheric
22 nanoparticles in the high Arctic, *Geophys. Res. Lett.*, 40, 3738-3743, 10.1002/grl.50661,
23 2013.

24 Kirkby, J., Curtius, J., Almeida, J., Dunne, E., Duplissy, J., Ehrhart, S., Franchin, A., Gagne,
25 S., Ickes, L., Kurten, A., Kupc, A., Metzger, A., Riccobono, F., Rondo, L., Schobesberger, S.,
26 Tsagkogeorgas, G., Wimmer, D., Amorim, A., Bianchi, F., Breitenlechner, M., David, A.,
27 Dommen, J., Downard, A., Ehn, M., Flagan, R. C., Haider, S., Hansel, A., Hauser, D., Jud,
28 W., Junninen, H., Kreissl, F., Kvashin, A., Laaksonen, A., Lehtipalo, K., Lima, J., Lovejoy, E.
29 R., Makhmutov, V., Mathot, S., Mikkila, J., Minginette, P., Mogo, S., Nieminen, T., Onnela,
30 A., Pereira, P., Petaja, T., Schnitzhofer, R., Seinfeld, J. H., Sipila, M., Stozhkov, Y.,
31 Stratmann, F., Tome, A., Vanhanen, J., Viisanen, Y., Vrtala, A., Wagner, P. E., Walther, H.,
32 Weingartner, E., Wex, H., Winkler, P. M., Carslaw, K. S., Worsnop, D. R., Baltensperger, U.,

1 and Kulmala, M.: Role of sulphuric acid, ammonia and galactic cosmic rays in atmospheric
2 aerosol nucleation, *Nature*, 476, 429-477, Doi 10.1038/Nature10343, 2011.

3 Korhonen, H., Carslaw, K. S., Spracklen, D. V., Mann, G. W., and Woodhouse, M. T.:
4 Influence of oceanic dimethyl sulfide emissions on cloud condensation nuclei concentrations
5 and seasonality over the remote Southern Hemisphere oceans: A global model study, *J.*
6 *Geophys. Res.-Atmos.*, 113, Artn D15204, Doi 10.1029/2007jd009718, 2008.

7 Kulmala, M., Pirjola, U., and Mäkelä, J. M.: Stable sulphate clusters as a source of new
8 atmospheric particles, *Nature*, 404, 66-69, 2000.

9 Kulmala, M., Vehkamäki, H., Petäjä, T., Dal Maso, M., Lauri, A., Kerminen, V. M., Birmili,
10 W., and McMurry, P. H.: Formation and growth rates of ultrafine atmospheric particles: a
11 review of observations, *J. Aerosol. Sci.*, 35, 143-176, 2004.

12 Kulmala, M., Kontkanen, J., Junninen, H., Lehtipalo, K., Manninen, H. E., Nieminen, T.,
13 Petäjä, T., Sipilä, M., Schobesberger, S., Rantala, P., Franchin, A., Jokinen, T., Järvinen, E.,
14 Äijälä, M., Kangasluoma, J., Hakala, J., Aalto, P. P., Paasonen, P., Mikkilä, J., Vanhanen, J.,
15 Aalto, J., Hakola, H., Makkonen, U., Ruuskanen, T., Mauldin, R. L., Duplissy, J., Vehkamäki,
16 H., Bäck, J., Kortelainen, A., Riipinen, I., Kurtén, T., Johnston, M. V., Smith, J. N., Ehn, M.,
17 Mentel, T. F., Lehtinen, K. E. J., Laaksonen, A., Kerminen, V.-M., and Worsnop, D. R.:
18 Direct Observations of Atmospheric Aerosol Nucleation, *Science*, 339, 943-946,
19 10.1126/science.1227385, 2013.

20 Küpper, F. C., Carpenter, L. J., McFiggans, G. B., Palmer, C. J., Waite, T. J., Boneberg, E.-
21 M., Woitsch, S., Weiller, M., Abela, R., Grolimund, D., Potin, P., Butler, A., Luther, G. W.,
22 Kroneck, P. M. H., Meyer-Klaucke, W., and Feiters, M. C.: Iodide accumulation provides
23 kelp with an inorganic antioxidant impacting atmospheric chemistry, *Proceedings of the*
24 *National Academy of Sciences*, 105, 6954-6958, 10.1073/pnas.0709959105, 2008.

25 Laaksonen, A., Kulmala, M., O'Dowd, C. D., Joutsensaari, J., Vaattovaara, P., Mikkonen, S.,
26 Lehtinen, K. E. J., Sogacheva, L., Dal Maso, M., Aalto, P., Petäjä, T., Sogachev, A., Yoon, Y.
27 J., Lihavainen, H., Nilsson, D., Facchini, M. C., Cavalli, F., Fuzzi, S., Hoffmann, T., Arnold,
28 F., Hanke, M., Sellegri, K., Umann, B., Junkermann, W., Coe, H., Allan, J. D., Alfarra, M. R.,
29 Worsnop, D. R., Riekkola, M. L., Hyotylainen, T., and Viisanen, Y.: The role of VOC
30 oxidation products in continental new particle formation, *Atmos. Chem. Phys.*, 8, 2657-2665,
31 2008.

1 Laborde, M., Schnaiter, M., Linke, C., Saathoff, H., Naumann, K. H., Möhler, O., Berlenz, S.,
2 Wagner, U., Taylor, J. W., Liu, D., Flynn, M., Allan, J. D., Coe, H., Heimerl, K., Dahlkötter,
3 F., Weinzierl, B., Wollny, A. G., Zanatta, M., Cozic, J., Laj, P., Hitzenberger, R., Schwarz, J.
4 P., and Gysel, M.: Single Particle Soot Photometer intercomparison at the AIDA chamber,
5 *Atmos. Meas. Tech.*, 5, 3077-3097, 10.5194/amt-5-3077-2012, 2012.

6 Laturnus, F.: Volatile halocarbons released from Arctic macroalgae, *Mar. Chem.*, 55, 359-
7 366, Doi 10.1016/S0304-4203(97)89401-7, 1996.

8 Lee, L. A., Carslaw, K. S., Pringle, K. J., and Mann, G. W.: Mapping the uncertainty in global
9 CCN using emulation, *Atmos. Chem. Phys.*, 12, 9739-9751, 10.5194/acp-12-9739-2012,
10 2012.

11 Lehtipalo, K., Kulmala, M., Sipila, M., Petaja, T., Vana, M., Ceburnis, D., Dupuy, R., and
12 O'Dowd, C.: Nanoparticles in boreal forest and coastal environment: a comparison of
13 observations and implications of the nucleation mechanism, *Atmos. Chem. Phys.*, 10, 7009-
14 7016, DOI 10.5194/acp-10-7009-2010, 2010.

15 Liu, P. S. K., Deng, R., Smith, K. A., Williams, L. R., Jayne, J. T., Canagaratna, M. R.,
16 Moore, K., Onasch, T. B., Worsnop, D. R., and Deshler, T.: Transmission Efficiency of an
17 Aerodynamic Focusing Lens System: Comparison of Model Calculations and Laboratory
18 Measurements for the Aerodyne Aerosol Mass Spectrometer, *Aerosol Sci. Technol.*, 41, 721-
19 733, 10.1080/02786820701422278, 2007.

20 Mahajan, A. S., Plane, J. M. C., Oetjen, H., Mendes, L., Saunders, R. W., Saiz-Lopez, A.,
21 Jones, C. E., Carpenter, L. J., and McFiggans, G. B.: Measurement and modelling of
22 tropospheric reactive halogen species over the tropical Atlantic Ocean, *Atmos. Chem. Phys.*,
23 10, 4611-4624, 10.5194/acp-10-4611-2010, 2010.

24 McFiggans, G., Coe, H., Burgess, R., Allan, J., Cubison, M., Alfarra, M. R., Saunders, R.,
25 Saiz-Lopez, A., Plane, J. M. C., Wevill, D. J., Carpenter, L. J., Rickard, A. R., and Monks, P.
26 S.: Direct evidence for coastal iodine particles from *Laminaria* macroalgae - linkage to
27 emissions of molecular iodine, *Atmos. Chem. Phys.*, 4, 701-713, 2004.

28 McFiggans, G., Alfarra, M. R., Allan, J., Bower, K., Coe, H., Cubison, M., Topping, D.,
29 Williams, P., Decesari, S., Facchini, C., and Fuzzi, S.: Simplification of the representation of
30 the organic component of atmospheric particulates, *Faraday Discuss.*, 130, 341-362, Doi
31 10.1039/B419435g, 2005.

1 McFiggans, G., Bale, C. S. E., Ball, S. M., Beames, J. M., Bloss, W. J., Carpenter, L. J.,
2 Dorsey, J., Dunk, R., Flynn, M. J., Furneaux, K. L., Gallagher, M. W., Heard, D. E.,
3 Hollingsworth, A. M., Hornsby, K., Ingham, T., Jones, C. E., Jones, R. L., Kramer, L. J.,
4 Langridge, J. M., Leblanc, C., LeCrane, J. P., Lee, J. D., Leigh, R. J., Longley, I., Mahajan,
5 A. S., Monks, P. S., Oetjen, H., Orr-Ewing, A. J., Plane, J. M. C., Potin, P., Shillings, A. J. L.,
6 Thomas, F., von Glasow, R., Wada, R., Whalley, L. K., and Whitehead, J. D.: Iodine-
7 mediated coastal particle formation: an overview of the Reactive Halogens in the Marine
8 Boundary Layer (RHAMBLe) Roscoff coastal study, *Atmos. Chem. Phys.*, 10, 2975-2999,
9 10.5194/acp-10-2975-2010, 2010.

10 Merikanto, J., Spracklen, D. V., Mann, G. W., Pickering, S. J., and Carslaw, K. S.: Impact of
11 nucleation on global CCN, *Atmos. Chem. Phys.*, 9, 8601-8616, 10.5194/acp-9-8601-2009,
12 2009.

13 Murray, B. J., Haddrell, A. E., Peppe, S., Davies, J. F., Reid, J. P., O'Sullivan, D., Price, H.
14 C., Kumar, R., Saunders, R. W., Plane, J. M. C., Umo, N. S., and Wilson, T. W.: Glass
15 formation and unusual hygroscopic growth of iodine acid solution droplets with relevance for
16 iodine mediated particle formation in the marine boundary layer, *Atmos. Chem. Phys.*, 12,
17 8575-8587, 10.5194/acp-12-8575-2012, 2012.

18 O'Dowd, C. D., Jimenez, J. L., Bahreini, R., Flagan, R. C., Seinfeld, J. H., Hämeri, K., Pirjola,
19 L., Kulmala, M., Jennings, S. G., and Hoffmann, T.: Marine aerosol formation from biogenic
20 iodine emissions, *Nature*, 417, 632-636, 2002.

21 O'Driscoll, P., Lang, K., Minogue, N., and Sodeau, J.: Freezing halide ion solutions and the
22 release of interhalogens to the atmosphere, *J Phys Chem A*, 110, 4615-4618, Doi
23 10.1021/Jp060491v, 2006.

24 Paatero, P., and Tapper, U.: Positive matrix factorization: A non-negative factor model with
25 optimal utilization of error estimates of data values, *Environmetrics*, 5, 111-126,
26 10.1002/env.3170050203, 1994.

27 Phinney, L., Leaitch, W. R., Lohmann, U., Boudries, H., Worsnop, D. R., Jayne, J. T., Toom-
28 Saunty, D., Wadleigh, M., Sharma, S., and Shantz, N.: Characterization of the aerosol over
29 the sub-arctic north east Pacific Ocean, *Deep-Sea Res. Pt. II*, 53, 2410-2433,
30 10.1016/j.dsr2.2006.05.044, 2006.

1 Riccobono, F., Schobesberger, S., Scott, C. E., Dommen, J., Ortega, I. K., Rondo, L.,
2 Almeida, J., Amorim, A., Bianchi, F., Breitenlechner, M., David, A., Downard, A., Dunne, E.
3 M., Duplissy, J., Ehrhart, S., Flagan, R. C., Franchin, A., Hansel, A., Junninen, H., Kajos, M.,
4 Keskinen, H., Kupc, A., Kürten, A., Kvashin, A. N., Laaksonen, A., Lehtipalo, K.,
5 Makhmutov, V., Mathot, S., Nieminen, T., Onnela, A., Petäjä, T., Praplan, A. P., Santos, F.
6 D., Schallhart, S., Seinfeld, J. H., Sipilä, M., Spracklen, D. V., Stozhkov, Y., Stratmann, F.,
7 Tomé, A., Tsagkogeorgas, G., Vaattovaara, P., Viisanen, Y., Vrtala, A., Wagner, P. E.,
8 Weingartner, E., Wex, H., Wimmer, D., Carslaw, K. S., Curtius, J., Donahue, N. M., Kirkby,
9 J., Kulmala, M., Worsnop, D. R., and Baltensperger, U.: Oxidation Products of Biogenic
10 Emissions Contribute to Nucleation of Atmospheric Particles, *Science*, 344, 717-721,
11 10.1126/science.1243527, 2014.

12 Saiz-Lopez, A., Plane, J. M. C., Baker, A. R., Carpenter, L. J., von Glasow, R., Martin, J. C.
13 G., McFiggans, G., and Saunders, R. W.: Atmospheric Chemistry of Iodine, *Chem. Rev.*, 112,
14 1773-1804, Doi 10.1021/Cr200029u, 2012.

15 Saiz-Lopez, A., Blaszczak-Boxe, C. S., and Carpenter, L. J.: A mechanism for biologically-
16 induced iodine emissions from sea-ice, *Atmos. Chem. Phys. Discuss.*, 15, 10257-10297,
17 doi:10.5194/acpd-15-10257-2015, 2015.

18 Saunders, R. W., Kumar, R., Martin, J. C. G., Mahajan, A. S., Murray, B. J., and Plane, J. M.
19 C.: Studies of the Formation and Growth of Aerosol from Molecular Iodine Precursor, *Z Phys*
20 *Chem*, 224, 1095-1117, DOI 10.1524/zpch.2010.6143, 2010.

21 Spracklen, D. V., Carslaw, K. S., Kulmala, M., Kerminen, V. M., Mann, G. W., and Sihto, S.
22 L.: The contribution of boundary layer nucleation events to total particle concentrations on
23 regional and global scales, *Atmos. Chem. Phys.*, 6, 5631-5648, 2006.

24 Sturges, W. T., Cota, G. F., and Buckley, P. T.: Bromoform Emission from Arctic Ice Algae,
25 *Nature*, 358, 660-662, Doi 10.1038/358660a0, 1992.

26 Sturges, W. T., Sullivan, C. W., Schnell, R. C., Heidt, L. E., and Pollock, W. H.:
27 Bromoalkane Production by Antarctic Ice Algae, *Tellus B*, 45, 120-126, DOI 10.1034/j.1600-
28 0889.1993.t01-1-00004.x, 1993.

29 Topping, D. O., McFiggans, G. B., and Coe, H.: A curved multi-component aerosol
30 hygroscopicity model framework: Part 1 - Inorganic compounds, *Atmos. Chem. Phys.*, 5,
31 1205-1222, 2005.

1 Ulbrich, I. M., Canagaratna, M. R., Zhang, Q., Worsnop, D. R., and Jimenez, J. L.:
2 Interpretation of organic components from positive matrix factorization of aerosol mass
3 spectrometric data, *Atmos. Chem. Phys.*, 9, 2891-2918, 2009.

4 Wang, M., Audi, G., Wapstra, A. H., Kondev, F. G., MacCormick, M., Xu, X., and Pfeiffer,
5 B.: The Ame2012 atomic mass evaluation, *Chinese Physics C*, 36, Artn 1603,
6 doi:10.1088/1674-1137/36/12/003, 2012.

7 Werner, A., and Kraan, S.: Review of the potential mechanisation of kelp harvesting in
8 Ireland, *Marine Environment & Health Series*, No.17, Marine Institute, Galway, 2004.

9 Whitehead, J. D., McFiggans, G. B., Gallagher, M. W., and Flynn, M. J.: Direct linkage
10 between tidally driven coastal ozone deposition fluxes, particle emission fluxes, and
11 subsequent CCN formation, *Geophys. Res. Lett.*, 36, L04806, 10.1029/2008GL035969, 2009.

12 Whitehead, J. D., Irwin, M., Allan, J. D., Good, N., and McFiggans, G.: A meta-analysis of
13 particle water uptake reconciliation studies, *Atmos. Chem. Phys.*, 14, 11833-11841, DOI
14 10.5194/acp-14-11833-2014, 2014.

15 Wiedensohler, A.: An Approximation of the Bipolar Charge-Distribution for Particles in the
16 Sub-Micron Size Range, *J. Aerosol. Sci.*, 19, 387-389, 1988.

17 Wiencke, C., and Amsler, C. D.: Seaweeds and their communities in polar regions, in:
18 *Seaweed Biology, Novel Insights into Ecophysiology, Ecology and Utilization*, edited by:
19 Wiencke, C., and Bischof, K., *Ecological Studies* 219, Springer, Berlin, Heidelberg, pp. 265–
20 291, 2012.

21 Williams, P. I., McFiggans, G., and Gallagher, M. W.: Latitudinal aerosol size distribution
22 variation in the Eastern Atlantic Ocean measured aboard the FS-Polarstern, *Atmos. Chem.*
23 *Phys.*, 7, 2563-2573, 2007.

24 Winklmayr, W., Reischl, G. P., Lindner, A. O., and Berner, A.: A New Electromobility
25 Spectrometer for the Measurement of Aerosol Size Distributions in the Size Range from 1 to
26 1000 nm, *J. Aerosol. Sci.*, 22, 289-296, 1991.

27 Yli-Juuti, T., Nieminen, T., Hirsikko, A., Aalto, P. P., Asmi, E., Horrak, U., Manninen, H. E.,
28 Patokoski, J., Dal Maso, M., Petaja, T., Rinne, J., Kulmala, M., and Riipinen, I.: Growth rates
29 of nucleation mode particles in Hyytiala during 2003-2009: variation with particle size,

1 season, data analysis method and ambient conditions, *Atmos. Chem. Phys.*, 11, 12865-12886,
2 DOI 10.5194/acp-11-12865-2011, 2011.

3 Yoon, Y. J., O'Dowd, C. D., Jennings, S. G., and Lee, S. H.: Statistical characteristics and
4 predictability of particle formation events at Mace Head, *J. Geophys. Res.-Atmos.*, 111,
5 D13204, 10.1029/2005JD006284, 2006.

6 Yu, F., and Luo, G.: Simulation of particle size distribution with a global aerosol model:
7 contribution of nucleation to aerosol and CCN number concentrations, *Atmos. Chem. Phys.*,
8 9, 7691-7710, 10.5194/acp-9-7691-2009, 2009.

9 Zhang, Q., Stanier, C. O., Canagaratna, M. R., Jayne, J. T., Worsnop, D. R., Pandis, S. N., and
10 Jimenez, J. L.: Insights into the chemistry of new particle formation and growth events in
11 Pittsburgh based on aerosol mass spectrometry, *Environ. Sci. Technol.*, 38, 4797-4809,
12 2004a.

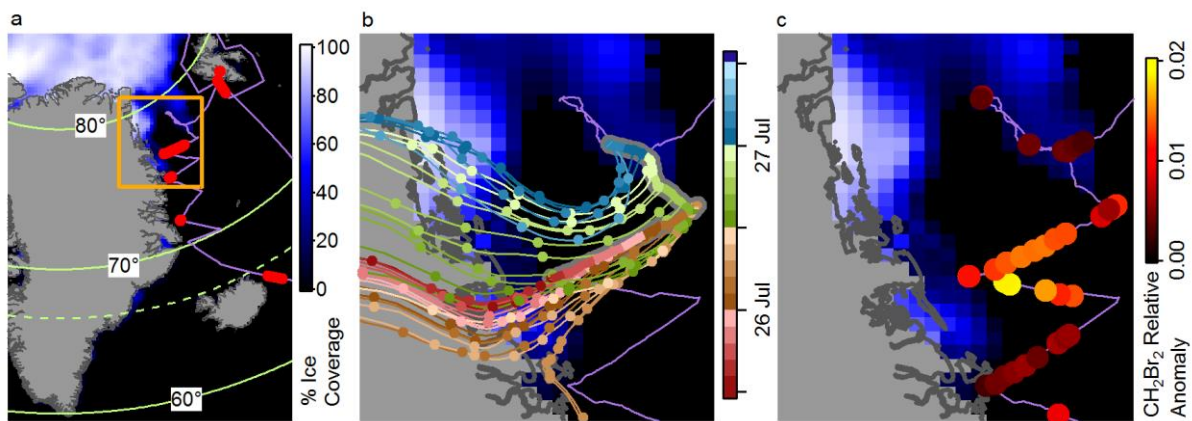
13 Zhang, X. F., Smith, K. A., Worsnop, D. R., Jimenez, J. L., Jayne, J. T., Kolb, C. E., Morris,
14 J., and Davidovits, P.: Numerical characterization of particle beam collimation: Part II -
15 Integrated aerodynamic-lens-nozzle system, *Aerosol Sci. Technol.*, 38, 619-638,
16 10.1080/02786820490479833, 2004b.

17 Zorn, S. R., Drewnick, F., Schott, M., Hoffmann, T., and Borrmann, S.: Characterization of
18 the South Atlantic marine boundary layer aerosol using an aerodyne aerosol mass
19 spectrometer, *Atmos. Chem. Phys.*, 8, 4711-4728, 2008.

20

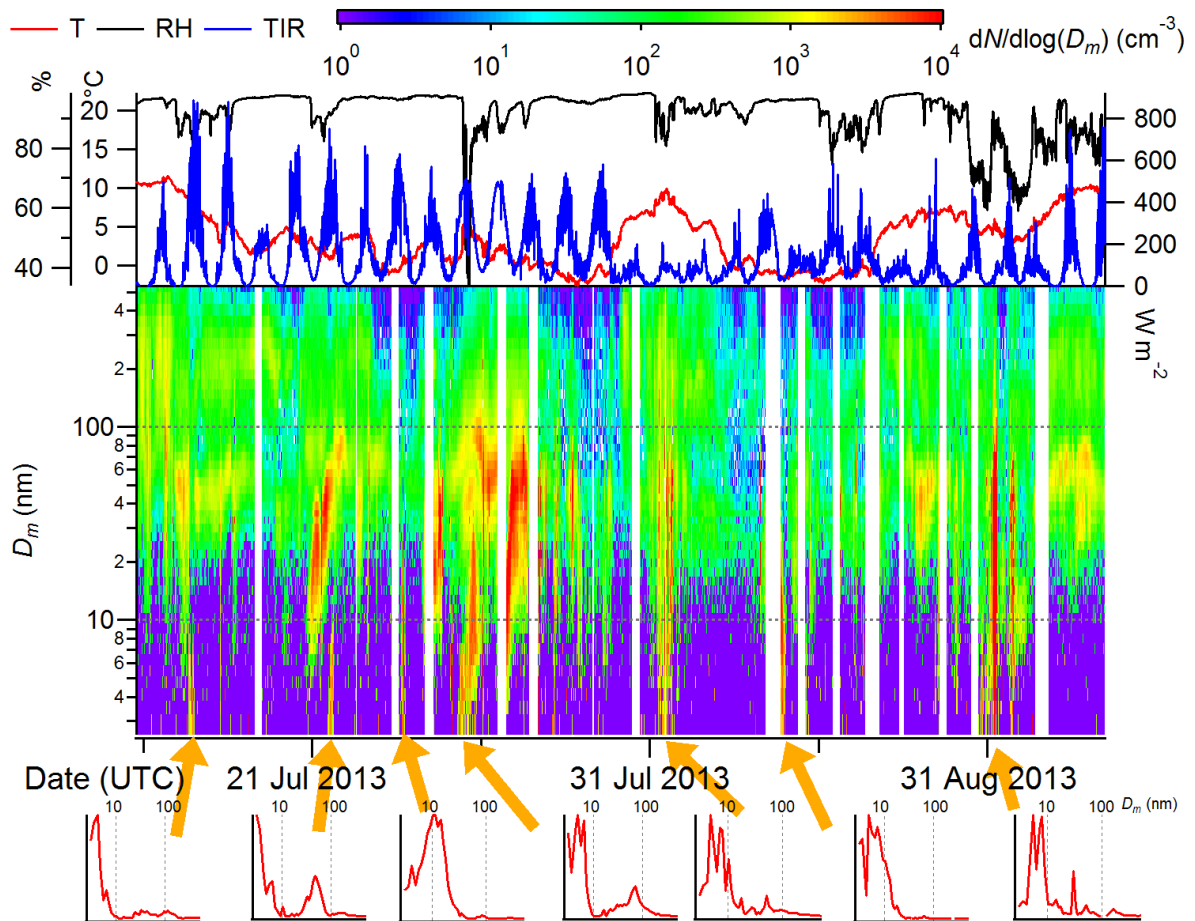
21

22



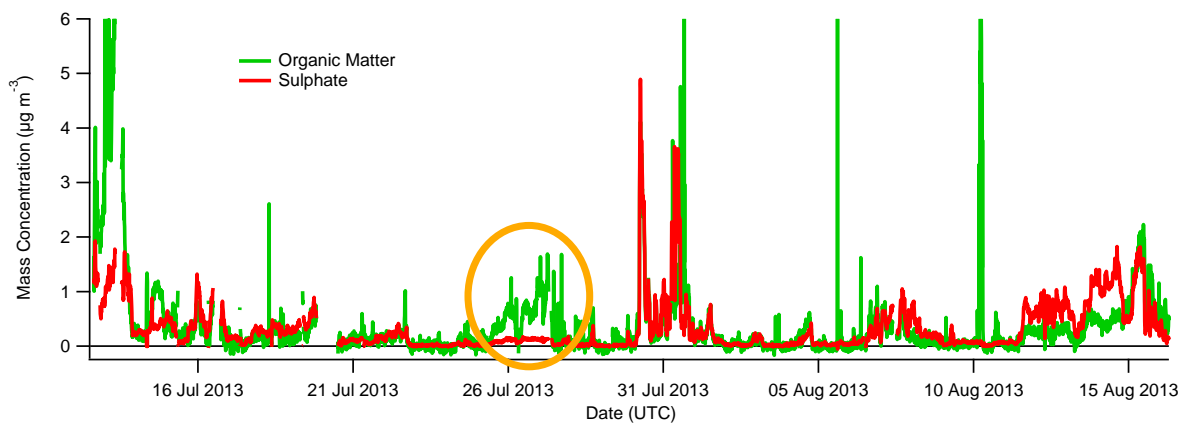
1
2
3
4
5
6
7
8
9

Figure 1: a) Cruise track (purple), ice coverage and locations of NPF events (red), defined by the presence of a mode of particles smaller than 10 nm not attributable to combustion or ship emissions (parts of the cruise outside of the area depicted did not show evidence of NPF). b) HYSPLIT back trajectories from cruise track corresponding to the 25-27 July case study. Markers are at 6-hourly intervals. c) Ratio of atmospheric concentrations of CH₂Br₂ (a product of ice diatom activity) to its saturation levels in seawater.



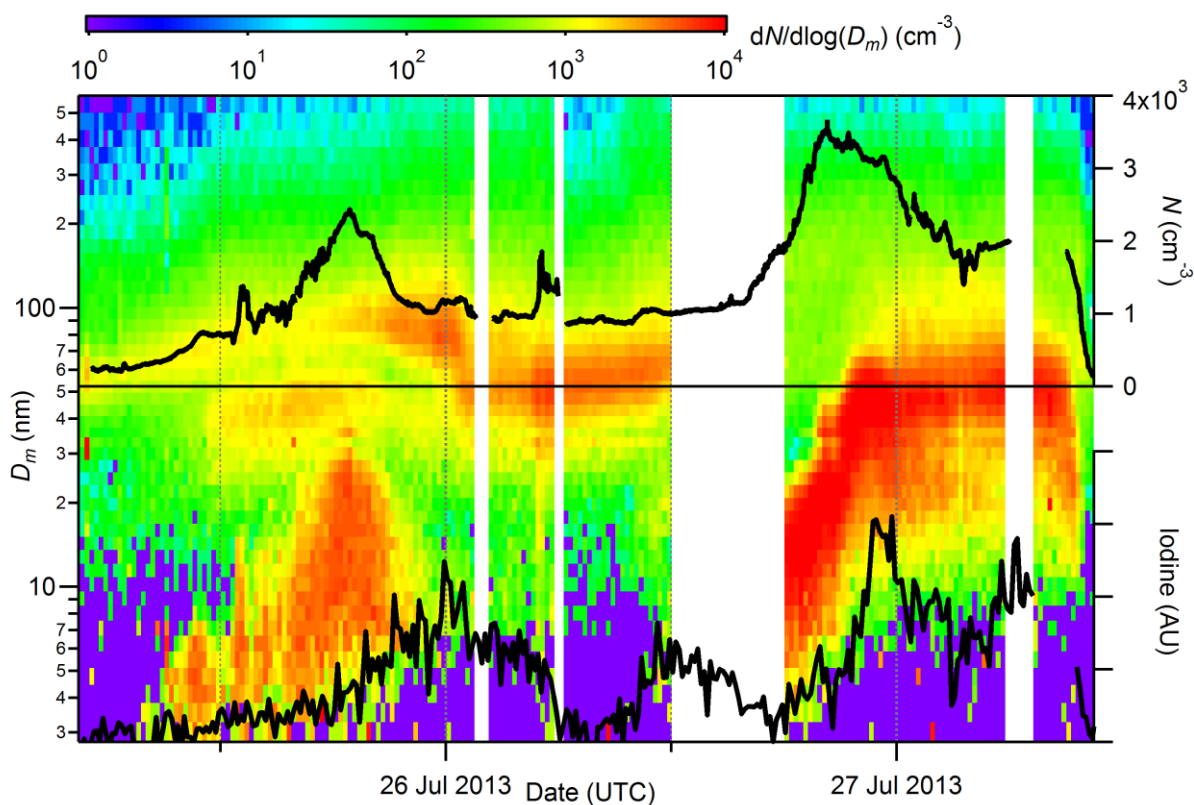
1
2
3
4
5
6
7
8
9
10

Figure 2: Temperature (T), relative humidity (RH) and total incident radiation (TIR) during the cruise, with DMPS size-resolved number concentration plotted data against electrical mobility diameter (D_m). White areas on the plot denote instrument downtime or when it was otherwise not sampling ambient air. Distributions from the seven candidate events in Fig. 1 are shown below to illustrate the shapes of the distributions during these events. Axis labels have been omitted for clarity, but are the same as the plot above, i.e. $dN/d\log(D_m)$ (cm^{-3}) vs D_m (nm).



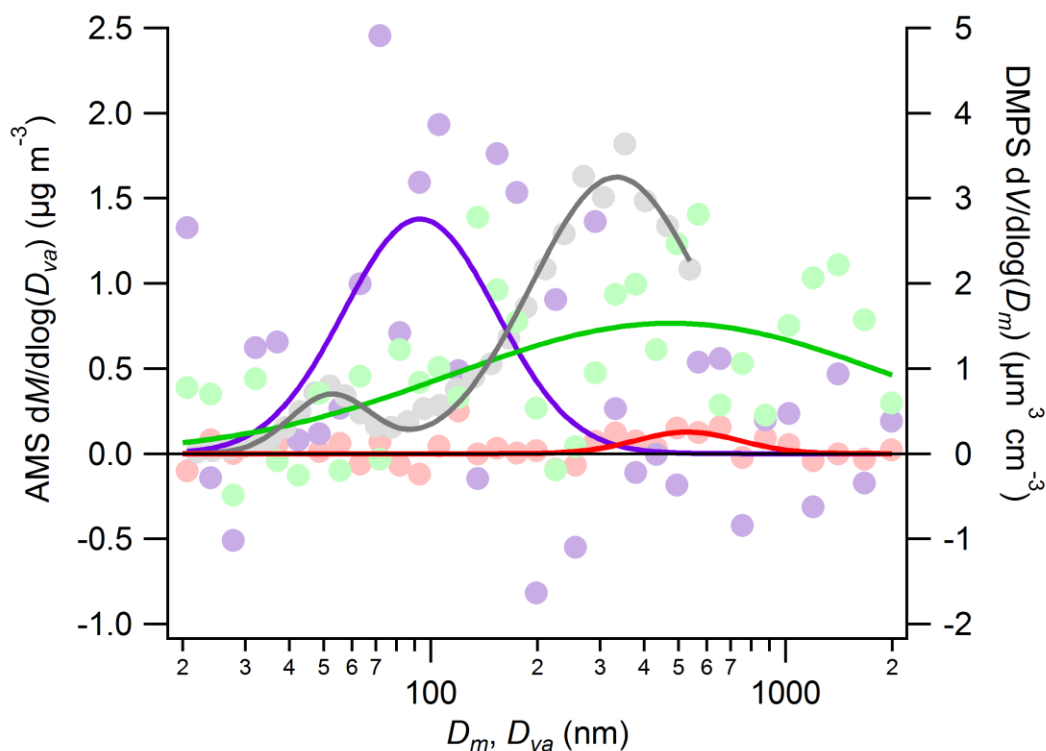
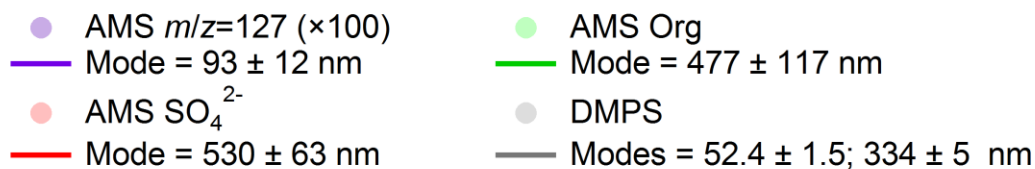
1
2
3
4
5
6
7
8
9

Figure 3: AMS-derived organic and sulphate mass concentrations, as calculated using the standard fragmentation tables (see section S2). Other commonly-reported species (nitrate and ammonium) were below detection limit outside of areas in close proximity to ports in the UK or Svalbard and thus considered irrelevant. The period of the main case study is highlighted in orange.

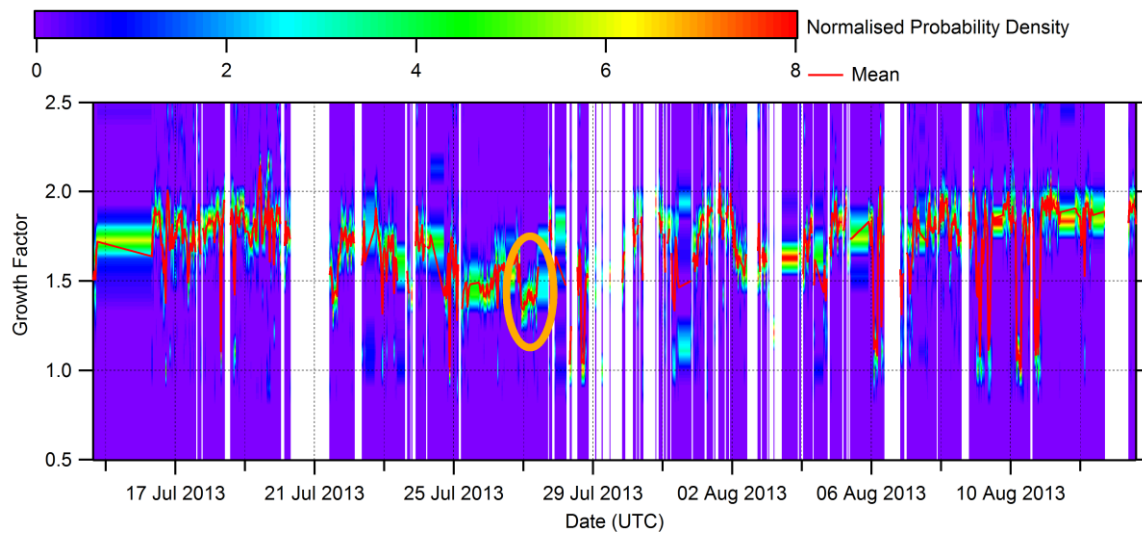


1
2
3
4
5
6
7
8
9

Figure 4: Size-resolved number concentrations ($dN/d\log(D_m)$) from a differential mobility particle sizer (DMPS) as a function of electrical mobility diameter (D_m), total number concentrations (N) from a condensation particle counter (CPC) and uncalibrated iodine ion concentrations from an Aerosol Mass Spectrometer (AMS) based on the signal at $m/z=127$ (I^+) during the main case study. White areas in the DMPS data show periods of ship influence or when the instrument was not sampling ambient air.



1
2
3 Figure 5: Size-resolved data from the DMPS and AMS, against electrical mobility and
4 vacuum aerodynamic diameters respectively, during the period of highest iodine loading (26
5 July 22:50-23:45 UTC) with lognormal nonlinear least squares fits and associated standard
6 errors, comparing DMPS volume with AMS mass at $m/z=127$, corresponding to I^+ , and
7 sulphate and organic matter. The low signal-to-noise ratios of the AMS data are due to the
8 low concentrations and short averaging time. Note that the widths of the AMS distributions
9 should not be directly compared against the DMPS, as the AMS distributions are subject to
10 broadening introduced by the chopper wheel and variations in particle density.
11



1
 2 Figure 6: HTDMA-derived growth factor probability distribution functions for 50 nm dry
 3 particles at 90 % relative humidity, with associated mean growth factors. The low growth
 4 factors associated with the case study time period (26 July 22:50-23:45) are highlighted.

5
 6
 7
 8
 9